Comparison of Theory and Experiment for Moments Induced by Loose Internal Parts

William P. D'Amico Jr.*
U.S. Army Ballistic Research Laboratory, Aberdeen Proving Ground, Maryland

Spin-stabilized projectiles often employ internal parts that are loose. Typical examples are safety mechanisms within fuzes, payload components, or submunitions. A series of tests were conducted where a loose internal part was driven by the rotor of a freely gimballed gyroscope. The motion of the loose part is not identical to that of the gyroscope and will cause the gyroscope yaw to grow. The gyroscope yaw history and the orbital motion of the loose part were measured to determine the phase angle between the motion of the loose part and the yawing motion of the gyroscope. The experimental data were used as input parameters to a theory that predicts moments (and, therefore, the yaw growth rate) induced by a loose internal part. Where the assumptions of the theory were appropriately modeled by the experiment, comparisons of theoretical and experimental yaw growth rates were consistent.

Nomenclature

K_1 = fast precessional amplitude
I_{ab}, I_{ac} = axial (spin) moments of inertia of the gyroscope body and component, respectively
I_{tb}, I_{tc} = transverse moments of inertia of the gyroscope body and component, respectively
I_a = $I_{ab} + I_{ac}$
I_t = $I_{tb} + I_{tc} + m_b x_b^2 + m_c x_c^2$
m_b, m_c = masses of the body and component, respectively
x_b, x_c = axial distances between the gyroscope *cm* and the body *cm* or the component *cm*
p, p_c = gyroscope spin, component spin
σ = $(1 - 1/s_g)^{1/2}$, where s_g is the gyroscopic stability factor
$\dot{\phi}_{1r}$ = fast precessional frequency for a rigid gyroscope = $(I_a/2I_t)(1+\sigma)p$
$\dot{\phi}_{2r}$ = slow precessional frequency for a rigid gyroscope = $(I_a/2I_t)(1-\sigma)p$
λ, λ_t = yaw damping, tare damping

Introduction

Background

MODERN projectile systems typically have fuze, submunition, or payload components that are not rigidly fixed. For example, small caliber ammunition often employ fuzes with safe and arming devices that utilize a spherical rotor. This rotor reduced the fast-mode precessional damping characteristics of the projectile system.[1-3] In another case, an artillery projectile experienced high yaw levels and large spin decays.[4] Presently, improved convention munitions (ICM) systems carry base-ejected submunitions and canisters. These payloads must be assembled and keyed with the projectile body, although small amplitude, internal motions are still possible.

Analytical investigations by Murphy[5,6] have explained much of the phenomena that was observed in Refs. 1-4; and he has provided fundamental models that predict the magnitudes of the yaw and spin moments induced by loose internal parts. Experimental tests using a spin fixture were performed by Bush to determine the despin moments produced by a loose ring on a circular shaft.[7] The experiments by Bush did not attempt to measure the motion of the loose part or to determine the phase angle between the motion of the spin fixture and the coning of the loose part. Hence, nominal values for the phase angle and the radial orbit were assumed in order to make comparisons between the experimental data and the theory.

The model suggested by Murphy assumes that the motion of the projectile has both slow and fast precessional modes. These two motions are decoupled and treated in a quasi-linear fashion. For practical applications, the motion is normally restricted to only the fast precessional mode (this corresponds with yawsonde-determined flight data). Within this model, the motion of the loose part must be assumed; then the response of the projectile system is determined. Two types of motion for the loose part were considered: 1) a forced precession about its own spin axis at the precession frequency of the projectile; or 2) a circulation motion of the mass center of the loose part at the precession frequency of the projectile.

If the loose part center-of-mass (*cm*) motion has a radius ϵ and a phase angle ϕ_ϵ with respect to the angle-of-attack plane, and the precessional motion has a cone angle γ and a phase angle ϕ_γ with respect to the angle-of-attack plane, then the relations for the fast precessional frequency ($\dot{\phi}_1$), the fast precessional damping (λ), and the change in the spin moment (ΔM_{spin}) are as follows:[6]

$$\dot{\phi}_1/\dot{\phi}_{1r} = 1 - C_1/[K_1(2I_t\dot{\phi}_{1r} - L_{a0})] \tag{1}$$

$$(\lambda - \lambda_t)K_1 = \dot{\phi}_1 S_1/(2I_t\dot{\phi}_1 - L_{a0}) \tag{2}$$

$$\Delta M_{\text{spin}} = -\dot{\phi}_1 K_1 S_1 \tag{3}$$

$$L_{a0} = I_{ab}p + I_{ac}p_c \tag{4}$$

$$S_1 = (I_{ac}p_c - I_{tc}\dot{\phi}_1)\gamma \sin\phi_\gamma - m_c x_c \dot{\phi}_1 \epsilon \sin\phi_\epsilon \tag{5}$$

$$C_1 = (I_{ac}p_c - I_{tc}\dot{\phi}_1)\gamma \cos\phi_\gamma - m_c x_c \dot{\phi}_1 \epsilon \cos\phi_\epsilon \tag{6}$$

It is important to note that the initial or starting motion for the projectile or the loose part is not considered within Refs. 5 and 6. Also, if the motion of the loose part is not at

Presented as Paper 85-1826 at the AIAA 12th Atmospheric Flight Mechanics Conference, Snowmass, CO, Aug. 19-21, 1985; received Aug. 26, 1985; revision received April 30, 1986.

*Mechanical Engineer, Launch and Flight Division. Member AIAA.

the precessional frequency of the projectile, then a prediction of yaw or spin moments is not possible. The amplitudes and phase angles of the assumed motions must be provided as inputs to the theory. If these are not known, then nominal values must be chosen. Previously, maximum physical clearances or tolerances were selected to determine the orbits, while phase angles of 90–45 deg were assumed.

A freely gimballed gyroscope was used as a test platform to conduct PRIM tests. A large series of tests were performed;[8,9] however, this report will primarily consider comparisons between round shaft experiments and theory. In the present experiments, the orbital motion and phase angle were measured directly. These, as well as other measured quantities, were used as inputs to the theory to provide a comparison between experiment and theory.

Initial Concepts for the Gyroscope Experiment

For the purposes of this experiment, it is assumed that a freely gimballed gyroscope will produce angular motions that realistically simulate the yawing motion of a projectile about its trajectory. The loose part is partially restrained within the gyroscope and will be referred to as the PRIM (partially restrained internal member). The motion of the PRIM within a gyroscope may have many components, but logically it will attempt to move independently as a gyroscope within a gyroscope or to respond as a forced oscillator to the motion of the gyroscope. Assuming the PRIM is forced to rotate at the spin frequency of the gyroscope, the following types of motion can exist:

1) Precessional motion based upon the PRIM inertial properties;

2) Circular motion of the PRIM *cm* at the spin frequency;

3) Precessional motion of the PRIM at the gyroscope precession frequency; and

4) Circular motion of the PRIM *cm* at the gyroscope precession frequency.

It is important to recall that the theoretical model[5,6] only considers the last two types of motion. This is reasonable since it is anticipated that only these types of motion would destabilize the precessional (or yawing) motion. PRIM motion at other frequencies would require subharmonic or ultraharmonic responses.[10] During the course of the gyroscope experiments, however, all four types of behavior were observed.

Description of Gyroscope

Figure 1 shows a schematic of the gyroscope (without support base), important instrumentation locations, and a physical coordinate system. Figure 2 shows a sectioned view of the gyroscope/PRIM model. Flexural pivots were used within the gimbal system and were instrumented with strain gages. The yaw amplitude was calibrated as a function of the output voltage of a bridge circuit. The orbit of the PRIM was monitored by noncontact inductive sensors (commonly called displacement transducers) that were mounted within the inner gimbal frame. The shaft and PRIM were driven by a DC motor, which was mounted below the inner gimbal. The spin of the shaft and PRIM remained constant during a data trial. Even under an open loop condition, despin of the rotor/PRIM assembly was not observed during the data trials. The precessional frequency of the gyroscope was controlled through the placement of nonspinning weights on a stem that was mounted to the top of the inner gimbal (shown in Fig. 2). The position of these weights determined the transverse moment of inertia of the gyroscope (I_t). The fast precessional frequency of the gyroscope was controlled by the selection of I_t. The axial moment of inertia (I_a) was a constant.

The damping of the flexural pivots within the gimbals and the location of the *cm* of the gyroscope produces a motion that is dominated by the fast precessional mode ($\dot{\phi}_1/p$ is approximately I_a/I_t). During the course of the experiments, some slow mode precession was observed, but this motion was rapidly damped when the fast precessional mode became unstable. Hence, for simplicity, the terminology "fast precession" will be abbreviated to "precession" or "yaw."

Data Reduction Techniques

The length and character of the data records required the use of both analog and digital reduction procedures. Often, data were reduced by two independent techniques to provide additional confidence.

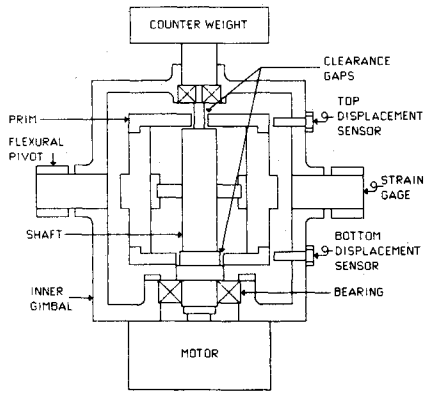

Fig. 2 PRIM gyroscope model.

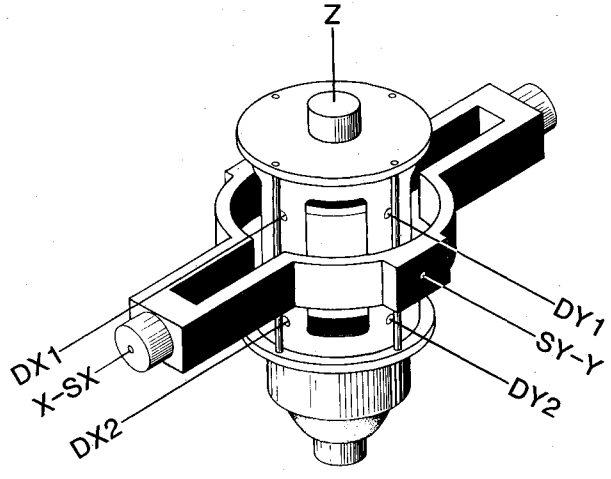

Fig. 1 Axis system and transducers for PRIM experiment.

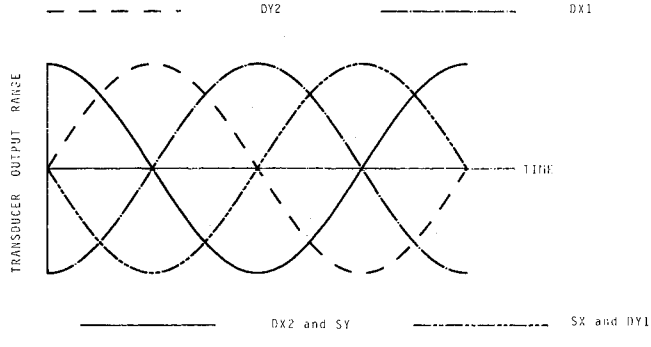

Fig. 3 Phase relations for $\phi_\gamma = 0$.

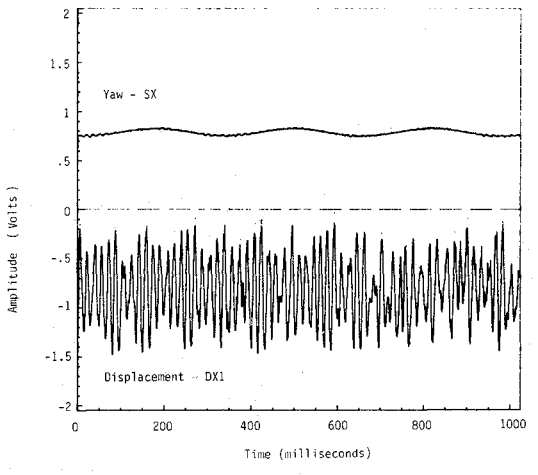

Fig. 4a Typical raw analog data for a round shaft at small yaw amplitudes ($p = 71.5$ Hz, $\dot{\phi}_1 = 3.31$ Hz).

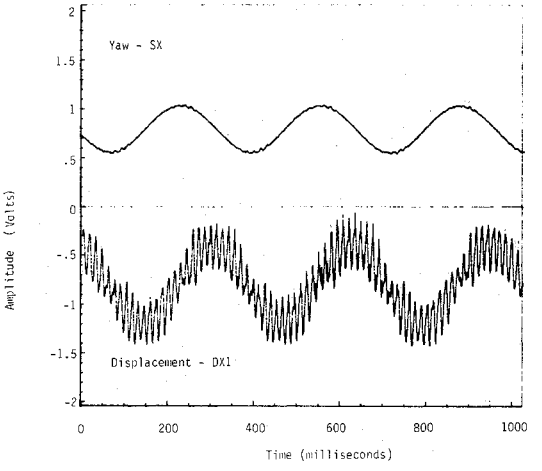

Fig. 5a Typical raw analog data for a round shaft at large yaw amplitudes ($p = 71.5$ Hz, $\dot{\phi}_1 = 3.31$ Hz).

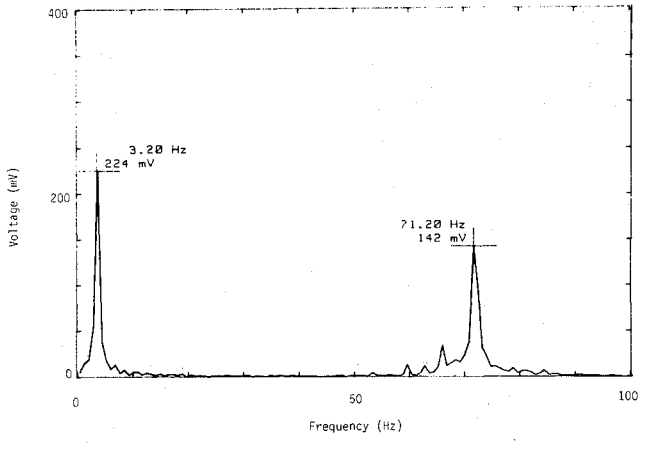

Fig. 4b Frequency spectrum for displacement transducer (DX1).

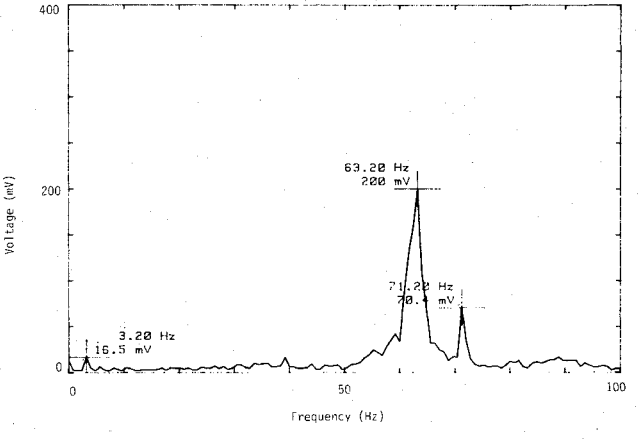

Fig. 5b Frequency spectrum for displacement transducer (DX1).

Yaw Data

The output of the flexural pivot/strain gage system gave a continuous projection of the yaw in the X and Y planes. The data in the Y plane were not reliable due to mechanical vibrations in the gimbals (probably excited by the motion of the PRIM). Normally, the data in the X plane (data from sensor SX) were reliable and were used. A series of data trials were conducted where the PRIM was fixed to the shaft. These tare runs were taken at various combinations of spin and precession frequencies to determine the natural yaw damping (λ_t) and the yaw frequency ($\dot{\phi}_{1r}$) of the total gyroscope/PRIM assembly when all the components were fixed. These tare data are required as inputs to Eqs. (1) and (2).

Both the tare and PRIM yaw data were reduced to obtain a log decrement type of growth rate. The yaw frequency was determined by the average number of zero crossings over several seconds of data. The data have not been processed to identify slow variations within the yaw frequency.

PRIM Motion Data

The orbit of the PRIM was continuously monitored by four displacement transducers; $DX1$ and $DX2$ in the XZ plane, and $DY1$ and $DY2$ in the YZ plane (as shown in Fig. 1). Sensors could also be mounted in the top support of the inner gimbal, but these positions were not normally utilized. Data from the displacement sensors were of very high quality and clearly indicated the motion of the PRIM. Typical outputs from a displacement transducer will be shown and discussed in following sections.

A primary objective of this PRIM experiment was to determine the phase angle between the yawing motion of the gyroscope and the motion of the PRIM. This phase angle was defined in Ref. 5 in terms of the two types of motion assumed in the model (phase angles for a precession of the PRIM [ϕ_γ] or for a *cm* motion of the PRIM [ϕ_ε]). Using these definitions, the natural phase relationships of all of the data transducers is shown in Fig. 3 for the special case of precession (no *cm* motion) when $\phi_\gamma = 0$. These inherent phase delays must be used to correct the raw data and to properly identify ϕ_γ.

The phase angle between the plane of the PRIM motion and the yaw plane must be determined in a convenient and reliable fashion. Data from three displacement transducers can be used to completely define the motion of the PRIM. However, this would require that the data be pre-processed or filtered to remove components of the motion not at the yaw frequency of the gyroscope. If the motion of the PRIM is well behaved, i.e., the motion is similar at all four displacement transducers, then the data from only one displacement transducer and a flexural pivot can be used to determine ϕ_γ. This can be accomplished by using a transfer function phase measurement between SX and $DX1$, for example. This phase measurement, when corrected by the relationships in Fig. 3, would then yield ϕ_γ. The transfer function could be obtained by analog or digital methods. It was convenient to use a Hewlett-Packard 3582A spectrum analyzer (SA) for phase measurements. The SA provides the phase across the entire frequency bandwidth, which was typically selected as 100–0 Hz (since the spin was less than 100 Hz). This type of measurement requires a sampling time of 5 s to determine the phase and to perform anti-aliasing func-

Table 1 Physical characteristics for the gyroscope/PRIM test[a]

I_t = transverse moments of inertia of fixed parts, kg·cm^2

Counterweight position	I_x	I_y
Top	1,935	1,879
Middle	1,777	1,717
Bottom	1,613	1,559

I_a = axial moment of inertia of fixed parts, kg·cm^2 = 0.737

$I_{t_{PRIM}}$ = transverse moment of inertia of the PRIM, kg·cm^2 = 87.1

$I_{a_{PRIM}}$ = axial moment of inertia of the PRIM, kg·cm^2 = 74.0

tions. The accuracy of the phase angles obtained with the *SA* is ±5 deg. It is possible to increase the length of the time record to compute an "averaged phase" for that given sampling period. It is highly probable that the gyroscope/PRIM parts produce a yaw growth rate that is based upon an average rather than instantaneous phase angle. Hence, this scheme for the determination of phase is quite realistic. Also, "instantaneous phase" measurements were made by digitizing and plotting both the yaw and displacement data and measuring the time delay between the wave forms to obtain the phase. Comparisons of the phase using these two techniques were consistent.

The physical and inertial characteristics of the gyroscope/PRIM parts were measured at the BRL Transonic Range and are given in Table 1.

The differences between I_x and I_y were assumed to be small, and the gyroscope was assumed to have a single transverse moment of inertia ($I_t = [I_x + I_y]/2$) for a particular counterweight position. The overall length of the PRIM was 12.7 cm (5 in.), and the PRIM *cm* was essentially at the geometric center. Note that the PRIM is almost an inertial sphere, i.e., $I_{a\text{PRIM}}/I_{t\text{PRIM}} = 0.850$.

The tare data were usable only at low spin rates. At spin frequencies of about 75 Hz, mechanical vibrations occurred, and the tare damping values were not used. (The PRIM that was temporarily shimmed and glued to a round shaft had become loose at these higher spin rates.) Trends from lower spin rate data were extrapolated for higher spin rates. The ratio of the rigid body (or tare) coning and spin frequencies ($\dot{\phi}_{1r}/p$) should be approximately equal to I_a/I_t, if the gravity moment is small. For the counterweight located at the middle position, $I_a/I_t = 0.0429$. Measured values of $\dot{\phi}_{1r}$ and p (for $p > 70$ Hz) yielded an average value of 0.0435 for $\dot{\phi}_{1r}/p$. Hence, the PRIM experiment is very nearly independent of gravity.

Round Shaft Data

The round shaft data showed three distinct types of behavior. Only one of these types of motion is reasonably approximated by the theory. When the gyroscope was released at zero yaw with no disturbance, the motion of the PRIM was dominated by a precessional motion at its own ratio of moments of inertia. Very little of the total motion was at the gyroscope yaw frequency. Figures 4a and 4b show raw analog data for yaw and PRIM displacement and the associated frequency spectrum for the displacement transducer. Under these conditions, the dominant PRIM motion is that of a free gyroscope. The fast precessional frequency of the PRIM should be approximately $I_{x\text{PRIM}}/I_{y\text{PRIM}} \approx \dot{\phi}_{1\text{PRIM}}/p$. The frequency data from Fig. 4b (63.2/71.2 = 0.888) can be collaborated by using the moments of inertia data in Table 1 (74/87.1 = 0.850). The initial PRIM motion provides a destabilizing torque to the gyroscope, and in many instances, this small moment eventually resulted in yaw growth. At intermediate yaw levels, the response of the PRIM was essentially random and aperiodic. A transition between a free oscillator and a forced oscillator was in progress. When the yaw of the gyroscope was well established, the PRIM motion was then dominated by a precessional motion at the gyroscope coning frequency (as shown in Figs. 5a and 5b). During this final stage of behavior, some of the PRIM motion was still at the spin frequency. The time-dependent motion of the PRIM (in frequency content and growing orbit) is more complex than the steady motions assumed within Ref. 5. Although these experiments were conducted using a free gyroscope and with no initial disturbance, the intent was to determine the steady motion of the PRIM if possible. This required long experiment run times in many instances. It is highly probable that impulsive launch and free-flight motion would generate only the final stages of PRIM motion, as observed within these tests. Future tests should be conducted to evaluate this assumption, however. The transient details of the PRIM motion were not addressed since "nominally steady" PRIM behavior was observed at relatively small levels of yaw for many of the experiments. For comparisons between theory and experiment, it will be necessary to separate the individual motion components by frequency. Only the motion component at the gyroscope yaw frequency should be compared to the theory. The data in Fig. 6a are typical of the final stage of motion. Raw (dashed line) and low passed (solid line) data are superimposed to demonstrate that the digital filtering does not introduce phase delay.

When the PRIM motion had a frequency and form that was representative of the assumptions of the theory, a phase angle was determined. It is necessary to determine from the displacement data whether a precessional or a *cm* motion of

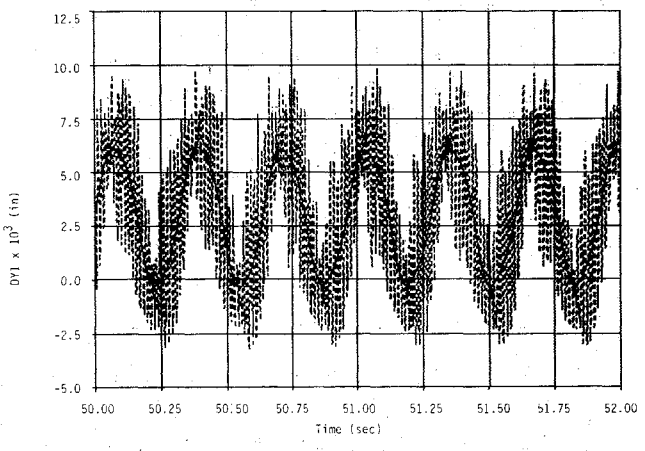

Fig. 6a Digitized DY1 data for run 4PO–raw and low pass filtered (10 Hz cut frequency).

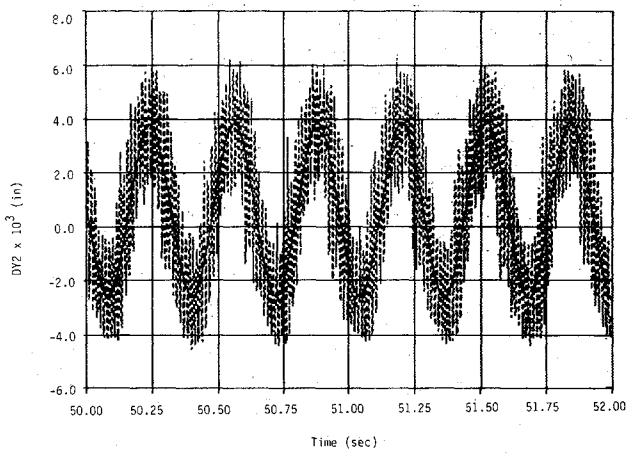

Fig. 6b Digitized DY2 data for run 4PO–raw and low pass filtered (10 Hz cut frequency).

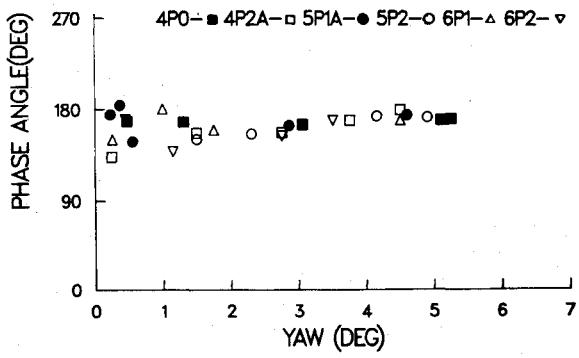

Fig. 7a Phase angle data for 0.005 in. round shafts.

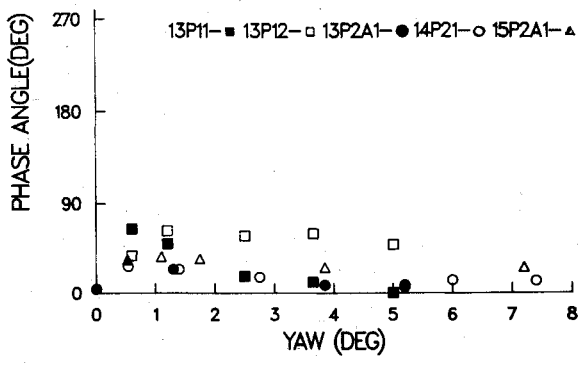

Fig. 7b Phase angle data for 0.005 in. octagon shaft.

the PRIM is present. If a *cm* motion exists (at a frequency of $\dot{\phi}_1$), then the displacement data from *DX*1 and *DX*2 (or *DY*1 and *DY*2) would be in phase. Figures 6a and 6b show data for *DY*1 and *DY*2 (raw and low pass filtered). These data are out of phase by 180 deg (as predicted by Fig. 3) and indicate that the PRIM motion is predominantly of a precessional type. The measured ϕ_γ values were typically between 150 and 170 deg. This was not expected, but is physically possible. Phase angles greater than 90 deg will increase the coning frequency of the gyroscope/PRIM system since Eq. (1) shows that the sign of the second term is controlled by $\cos(\phi_\gamma)$; this trend was observed. However, as previously stated, the resolutions of the frequency measurements were not sufficient to quantitatively compare experiment to theory. Figure 7a shows the variation of phase angle versus yaw amplitude for several of the round shaft experiments. The phase angle could have been plotted using time rather than yaw angle, but this would not have changed the character of the plot. Since yaw levels of less than 5 deg are typical for actual projectile flights, this figure indicates that relatively constant phase angles should be occurring during flight. The time-dependent behavior of the phase angle could be correlated against other parameters, such as yaw growth rate or precession frequency. This was not done since all of these parameters reflect some type of time-averaging. The primary intent was to determine the steady state value of the phase angle as an input to test the theory. Figure 7b shows phase angle data for octagonal shafts. The phase angles are less than 90 deg for all cases.

Comparisons Between Experiment and Theory

A realistic validation of the theory can be conducted by using the experimentally determined values of yaw growth rate, phase angle, and cant angle. Such comparisons have not been previously made and will be explained here. Equations (1) and (2) are restricted to a precessional motion of the PRIM. Within Eq. (2), the yaw growth rate and tare damping are combined into a single quantity and identified as the experimental yaw growth rate. The other remaining term within Eq. (2) is essentially the theoretical estimation of yaw growth rate (although it does require experimentally determined values of phase angle and cant angle). The experimental yaw growth rate can be nondimensionalized by the coning frequency. The dimensionless growth rates will be identified as ϵ_{exp} and ϵ_{theory}. The quantity $2\pi\epsilon_{exp}$ (or $2\pi\epsilon_{theory}$) is approximately the fractional change in K_1 (the yaw amplitude) for each cycle of the yaw frequency, $\dot{\phi}_1$. The loose part also affects the yaw frequency of the gyroscope/PRIM system. The change in the yaw frequency is presented as a ratio of the gyroscope/PRIM

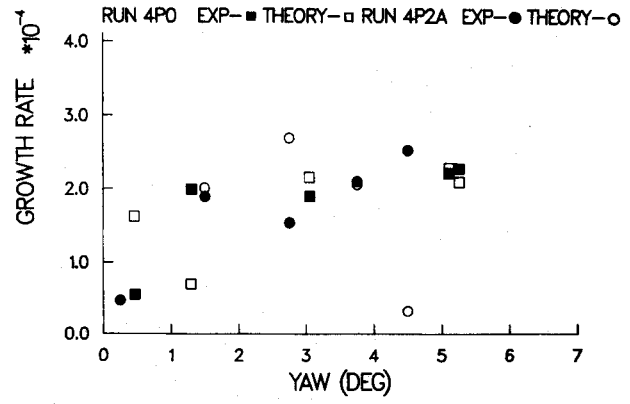

Fig. 8a Comparison of theory and experiment for 0.005-in. round shaft (runs 4PO and 4P2A).

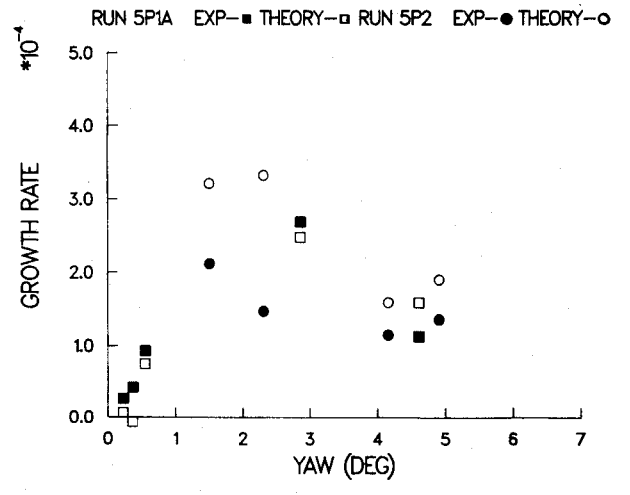

Fig. 8b Comparison of theory and experiment for 0.005-in. round shaft (runs 5P1A and 5P2).

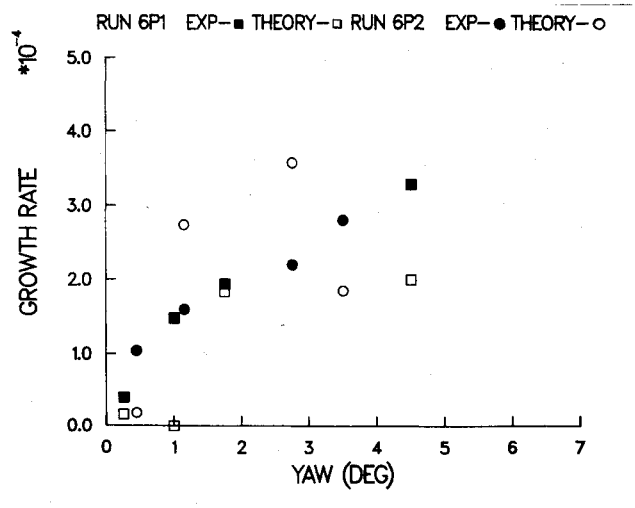

Fig. 8c Comparison of theory and experiment for 0.005-in. round shaft (runs 6P1 and 6P2).

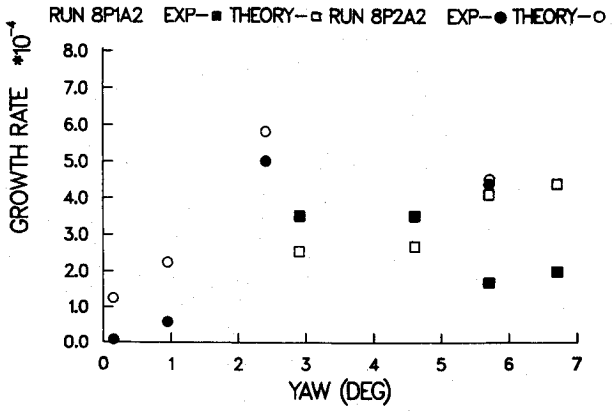

Fig. 8d Comparison of theory and experiment for 0.010-in. round shaft (runs 8P1A2 and 8P2A2).

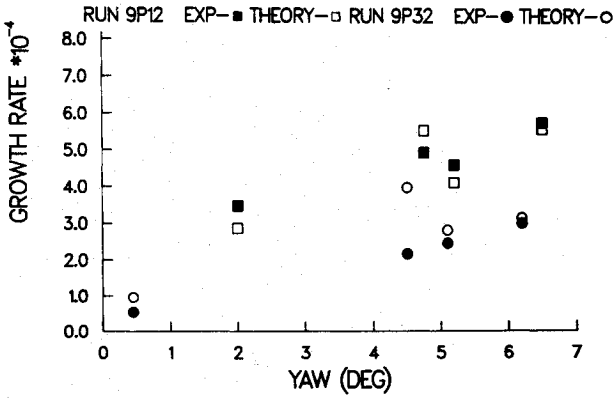

Fig. 8e Comparison of theory and experiment for 0.010-in. round shaft (runs 9P12 and 9P32).

frequency to the tare coning frequency, which is the rigid body coning frequency. As was the case with the yaw growth rate, the terms in Eq. (1) are separated into experimental and theoretical values and are presented as a ratio of the coning frequencies, $\dot{\phi}_1/\dot{\phi}_{1r}$. Normally, the observed $\dot{\phi}_1/\dot{\phi}_{1r}$ ratio was greater than unity for the round shafts and less than unity for the octagonal shafts. This reflects the phase angle behavior for the round shafts ($\cos\phi_\gamma < 1$) and for the octagonal shafts ($\cos\phi_\gamma < 1$). Hence, a qualitative comparison between theoretical and experimental $\dot{\phi}_1/\dot{\phi}_{1r}$ values reflects consistent behavior for the phase angle and the increase or decrease of the gyroscope coning frequency.

Figures 8a-8e show comparisons between round shaft theory and experiment. The first comparisons are for 0.005-in. shafts. The results shown in Fig. 8a are consistent at late times, as expected. Only the highest yaw level of Run 4P2A indicated poor agreement. However, a close examination of the data records indicate that the orbit of the PRIM shrank abruptly at this time. Hence, some type of unsteady behavior or noise was present. Differences of roughly 10% are observed. Orbit and phase angle data are relatively steady for these two runs. The comparisons in Fig. 8b show consistent trends for all amplitude levels, small and large. The agreement at very small yaw levels may be fortuitous since larger differences are observed for larger yaw levels (where the assumptions of the theory should be better approximated). The differences are larger here (25%) than for the previous runs. Figure 8c shows results that were similar to Fig. 8c, although the differences between experiment and theory are slightly larger (approximately 40% at the large yaw levels). The data records indicate that both the orbit and phase angle for these runs were not as yet steady; hence, poor agreement should be expected. The final two figures show comparisons for 0.010-in. shafts. Comparisons for Run 8P2A2 are consistent, while those for Run 8P1A2 were not. For this last case, the phase angle is constant, however, the orbit of the PRIM was not. The comparisons in Fig. 8e were very consistent.

Conclusions

A series of gyroscope experiments were conducted for a loose internal part. Detailed comparisons were made to a linearized and steady state theory. Comparisons were consistent when the assumptions of the theory were well modeled by the experiment. However, complex motions of the internal part were observed and were not considered in the present theory. Measurements of the radial orbit and the phase difference between the loose part motion and the gyroscope yaw were made through the use of noncontact transducers. Phase angle and radial orbit measurements showed that previously assumed nominal or maximum values for these quantities give overpredictions when used with available theory.

Acknowledgments

The author is indebted to Mr. Geoffrey Markovic for his patience and dedication in the reduction of the raw and final data. Most of the plots and data files used for plotting were generated by Mr. Markovic. Mr. Steven Kushubar provided excellent support on the Launch and Flight Division VAX 11/780. The experiment was conceptually designed in a joint effort by Lawrence Livermore National Laboratories (LLNL), Sandia National Laboratory, Albuquerque (SNLA), and the BRL. The hardware and instrumentation for the PRIM experiments were built and assembled by LLNL, while the tests were conducted by LLNL and BRL at the Launch and Flight Division, BRL.

References

[1]Boyer, E. D., "Comparison of Aerodynamic Characteristics of 20mm HEI Shell M97 with Fuze M75 and 20mm Shell T216E1 with Fuze M505," BRL MR-865, U.S. Army Ballistic Research Laboratories, Aberdeen Proving Ground, MD, April 1955.

[2]Boyer, E. D., "Aerodynamic Characteristics for Small Yaws of 20mm Shell, HEI, T282E1 with Fuze M505 for Mach Numbers .36 to 3.78," MR-916, U.S. Army Ballistic Research Laboratories, Aberdeen Proving Ground, MD, August 1955.

[3]Roecker, E. T. and Boyer, E. D., "Aerodynamic Characteristics of 30mm HEI Shell, T306E10," BRL MR-1098, U.S. Army Ballistic Research Laboratories, Aberdeen Proving Ground, MD, August 1957.

[4]Karpov, B. G. and Bradley, J. W., "A Study of Causes of Short Ranges of the 8" T317 Shell," BRL MR-1049, U.S. Army Ballistic Research Laboratories, Aberdeen Proving Ground, MD, May 1958.

[5]Murphy, C. H., "Influence of Moving Internal Parts on Angular Motion of Spinning Projectiles," *Journal of Guidance and Control*, Vol. 1, March-April 1978, pp. 117-122 (see also BRL MR-2731, Feb. 1977).

[6]Murphy, C. H., "Estimated Effect on Projectile Flight Stability of an Interior Cantilever Beam," BRL MR-03060, U.S. Army Ballistic Research Laboratory, Aberdeen Proving Ground, MD, Sept. 1980.

[7]Bush, Clarence C., "Inertial Despin Moment Measurements of a Canted Loose Ring During Spin and Nutation," BRL MR-03013, U.S. Army Ballistic Research Laboratory, Aberdeen Proving Ground, MD, April 1980.

[8]Morgan, T., "The Influence of Internal Moving Parts on the Ballistic Flight Path of a Projectile," AIAA Paper 85-1841, Aug. 1985.

[9]Cornell, R. H., "Experimental Investigation of Dynamic Motions of an Internal Part in an Artillery Projectile," AIAA Paper 85-1842, Aug. 1985.

[10]Stoker, J. J., *Nonlinear Vibrations*, John Wiley and Sons, New York, 1950.